IX CONGRESSO BRASILEIRO DE
ENGENHARIA E CIÊNCIAS TÉRMICAS

9th BRAZILIAN CONGRESS OF THERMAL
ENGINEERING AND SCIENCES

Paper CIT02-0174

Numerical Modeling of the Planetary Boundary Layer

Amauri Pereira de Oliveira
apdolive@usp.br

Jacyra Soares
jacyra@usp.br

Hugo A. Karam
hakaram@model.iag.usp.br

Maxsuel M. R. Pereira
maxsuel@model.iag.usp.br

Edson P. Marques Filho
emarques@model.iag.usp.br

Group of Micrometeorology, Department of Atmospheric Sciences, Institute of Astronomy, Geophysics and Atmospheric Sciences, University of São Paulo, Rua do Matão, 1226, 05508.900 - São Paulo, SP, Brazil.

Abstract. *This work describes the major available techniques to simulate the time and space evolution of the planetary boundary layer. For homogeneous and equilibrium conditions the structure of the planetary boundary layer can be diagnosed from the Monin-Obukhov, Free Convection, Local and Mixed Layer Similarity theories. For the other atmospheric conditions the planetary boundary layer can be numerically simulated using first and second order closure models and large eddy models. The closure models take into consideration the traditional statistical approach. Large eddy simulation models are based on the filtered equations of motion and require the statistical approach to estimate subgrid turbulence.*

Keywords *Numerical Modeling, Large eddy simulation; Convective boundary layer; Dispersion of inert pollutants, Planetary boundary layer*

1. Introduction

The Planetary Boundary Layer (PBL) is the region of the atmosphere, adjacent to the surface, where turbulence is the dominant feature. The intensity of turbulence determines the spatial distribution of thermodynamic and dynamic properties in the PBL as well as its vertical extent. Over continental areas, the turbulence is maintained by wind shear throughout the day, and it is intensified by thermal convection, during daytime, and restrained by surface inversion layer during nighttime. Its vertical extent varies from 300-1500 m, during day, to 100-300 m at night. Over the ocean the thermal effects on the turbulence is much less important and its vertical extent has smaller amplitude compare to the continental areas (Garrat, *et al.* 1996). Improving the understanding of PBL is important for several human activities: weather forecasting, pollution management, agriculture, etc. The PBL properties can be described by application of numerical and physical modeling. The numerical models are based on numerical solution of momentum, thermodynamic and mass conservation laws (Wyngaard, 1985). Physical modeling of the PBL is accomplished by wind tunnels and convection tank. (Plate, 1999; Cermark 1995; Lu and Arya, 1995; Avissar *et al*, 1990). In this paper the major techniques used to model numerically the PBL will be reviewed, and some numerical results will be shown.

2. PBL Models

Turbulent flow can be simulated numerically by solving directly the equations of motion discretized over a mesh (She, *et al.* 1991). The number of grid points required to describe a turbulent flow with characteristic length scale l is given by $(l/h)^3$, where h is the Kolmogorov microscale. It can be shown that the number of grid points is proportional to the Reynolds number (Re) of the flow according to the $(l/h)^3 \approx Re^{9/4}$. Applying direct numeric simulation (DNS) to simulate the PBL would require, for typical conditions $l = 1000\ m$ and $h = 0.001\ m$, about 10^{27} grid points. This simple result indicates that DNS cannot be applied to simulate PBL.

The turbulent flows can be (and have been) adequately described by statistical methods. The hypothesis is that each dynamic and thermodynamic properties of the flow can be treated as a random variable (Monin and Yaglon, 1971 Frisch, 1995). The concept of ensemble average, or Reynolds average, is than applied to derive the prognostic mean equations of motion necessary to describe the statistical properties of the PBL (Stull, 1988).

This work will focus on the PBL mean properties associated to the zonal and meridional components of the wind ($\overline{u}$,$\overline{v}$) and mean potential temperature ($\overline{q}$). The over bar indicates Reynolds average. The momentum and thermodynamic conservation laws applied to atmosphere can be simplified, considering the air as an ideal gas, resulting into a set of 3 equations as illustrated in Table 1. There, the symbols $-1/r_o(\partial \overline{p}/\partial y)$ and $-1/r_o(\partial \overline{p}/\partial x)$ indicate the horizontal mean pressure gradient acceleration in the x and y directions, where r_o is basic state atmospheric density; $-f\overline{v}$ and $-f\overline{u}$ are the Coriolis acceleration, where f is the Coriolis parameter; $\overline{(u'w')}$ and $\overline{(v'w')}$ are vertical turbulent fluxes of momentum; $\overline{(q'w')}$ is the vertical turbulent flux of sensible heat; $(-1/r_0 c_P)(\partial R_N/\partial z)$ is the vertical divergence of the net radiation flux, where c_P is the air specific heat at constant pressure. The thermodynamic equation is commonly expressed in terms of potential temperature, which is, by definition, the temperature that any air parcel would have if was brought adiabatically to the level pressure of 1000 hPa (p_{00}). It can be estimated by $q = T(p/p_{00})^{R/C_P}$, where T and p are the temperature and pressure of the air parcel and R_D is the dry air gas constant.

Table 1. The Reynolds averaged momentum and thermodynamic equations used to describe the atmosphere mean state of a horizontally homogeneous PBL.

	Equation	Unknown
1	$\frac{\partial \overline{u}}{\partial t} = -\frac{\partial \overline{(u'w')}}{\partial z} + \left(-\frac{1}{r_o}\frac{\partial \overline{p}}{\partial x} + f\overline{v}\right)$	$\overline{u}$ and $\overline{(u'w')}$
2	$\frac{\partial \overline{v}}{\partial t} = -\frac{\partial \overline{(v'w')}}{\partial z} + \left(-\frac{1}{r_o}\frac{\partial \overline{p}}{\partial y} - f\overline{u}\right)$	$\overline{v}$ and $\overline{(v'w')}$
3	$\frac{\partial \overline{q}}{\partial t} = -\frac{\partial \overline{(q'w')}}{\partial z} - \left(\frac{1}{r_0 c_P}\frac{\partial R_N}{\partial z}\right)$	$\overline{q}$ and $\overline{(q'w')}$

The advection terms in equation of motion (Table 1) are dropped because it is assumed that: (i) the PBL is homogeneous in the horizontal directions; (ii) the mean vertical velocity ($\overline{w}$) is equal zero. The accelerations associated to the horizontal component of pressure gradients, $-1/r_o(\partial \overline{p}/\partial x)$ and $-1/r_o(\partial \overline{p}/\partial y)$, are kept because they represent the external forcing associated to meteorological disturbances in spatial scales larger the ones used to consider the PBL horizontally homogeneous (Stull, 1988). Above the PBL, in the free atmosphere (Fig. 1) the turbulent flux are negligible, and the atmosphere is in geostrophic equilibrium, so that the horizontal wind can be represented by $u_g = -1/f r_o(\partial \overline{p}/\partial y)$ and $\overline{v}_g = +1/f r_o(\partial \overline{p}/\partial x)$, at least in the middle latitudes. Therefore, as the PBL evolves, the geostrophic equilibrium is disrupted by turbulent friction, $-\partial \overline{(u'w')}/\partial z$ and $-\partial \overline{(v'w')}/\partial z$, which decelerates the horizontal components of the mean wind.

The temporal and spatial evolution of potential temperature in the free atmosphere is given by the radiation cooling or heating. In the PBL, the divergence of turbulent sensible heat, $-\partial \overline{(q'w')}/\partial z$, will warm up the lower atmosphere, during daytime, and cool down, during nighttime, as result of the daytime solar heating of the surface and long wave radiation cooling during nighttime, respectively. It should be emphasized that the set of equations in Table 1 implies also that the mean flow, in the vertical direction, is in hydrostatic balance expressed by: $g = -1/r_o(\partial \overline{p}/\partial z)$, where g is the gravity acceleration. The set of motion equation in Table 1 reflects also the Boussinesq approximation, where the mean flow is non-divergent, $\partial \overline{u}/\partial x + \partial \overline{v}/\partial y + \partial \overline{w}/\partial z = 0$, the equation of state is given by $\overline{r}/r_0 = -\overline{q}/q_0$, with q_0 being the basic state atmospheric potential temperature. The basic state is also assumed to obey the ideal gas law $p_0 = r_o R_D T_0$ (Dutton and Fitchl, 1969, Mahrt, 1986). The resulting set of equations used to describe the mean state suffers from the closure problem - the number of unknowns is larger than the number of equations (Table 1). To overcome the closure problem four approaches have been developed: (a) similarity laws; (b) bulk model, (c) first and superior order closure schemes and (d) Large eddy simulation models.

2.1. Similarity Laws

The similarity laws are derived from the observational fact that under certain conditions, the turbulence is intense enough to adjust itself to surface and the external forcing changes fast enough so that the statistical properties of the PBL are of equilibrium. Under this rather frequent condition the PBL properties are self-similar when normalized by appropriated characteristic scales. In the PBL, *Monin-Obukhov, Free Convection, Mixed Layer* and *Local (or Z-less)* are similarities most celebrated by use (Sorbjan, 1989).

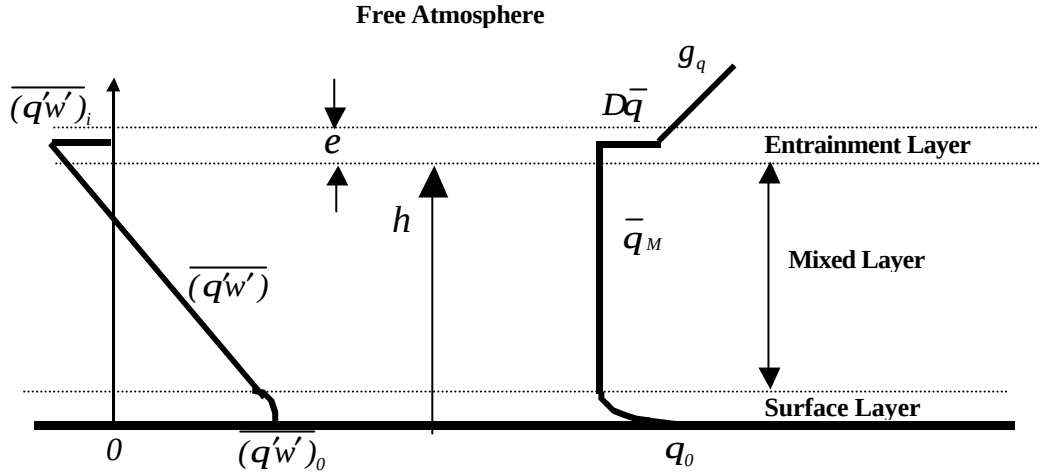

Figure 1: Schematic description the bulk model thermodynamic structure for convective PBL. The vertical extent of the PBL is indicated by h. The PBL potential temperature in the mixed layer is constant and indicated by $\bar{q}_M$. The potential temperature at the surface is indicated by $\bar{q}_0$. The intensity of temperature inversion at the top of the mixed layer is given by $D\bar{q} = \bar{q}(h+e/2) - \bar{q}_M$, where e is the depth of the entrainment layer. Above the PBL, the vertical rate of potential temperature variation is indicated by g_q. The turbulent sensible heat flux varies linearly across the mixed layer from $\overline{(q'w')}_0$, in the surface layer, to $\overline{(q'w')}_i$, in the entrainment layer.

They are known as similarity laws and are based on a set of empirical expressions developed to diagnose statistic properties of the turbulent flow wind velocity [$\bar{V} = \sqrt{\bar{u}^2 + \bar{v}^2}$], variances of the wind components [$s_u^2 = \left(\overline{(u'u')} + \overline{(v'v')} + \overline{(w'w')}\right)$, $s_v^2 = \left(\overline{(u'u')} + \overline{(v'v')} + \overline{(w'w')}\right)$, $s_w^2 = \left(\overline{(u'u')} + \overline{(v'v')} + \overline{(w'w')}\right)$], variance of potential temperature [$s_q^2 = \overline{(q'q')}$], co-variances [$\overline{(u'w')}$, $\overline{(v'w')}$, $\overline{(q'u')}$, $\overline{(q'v')}$, $\overline{(q'w')}$] as well as their spectral and co-spectral distribution in the frequency space.
The Monin-Obukhov and free convection similarities are valid for the surface layer (SL, Fig. 1) and for stability conditions typically observed in this PBL layer. The characteristic scales of wind, temperature and length are respectively, u_*, q_*, z and L for the Monin-Obukhov and u_F, q_F and z for free convection (Table 2)

Table 2: Characteristic scales used in the Monin-Obukhov and Free Convection similarity valid for the Atmospheric Surface Layer.

Characteristic Scale	Monin-Obukhov	Free Convection
Wind Velocity	$u_* = \sqrt[4]{\overline{(u'w')}_o^2 + \overline{(u'w')}_0^2}$	$u_F = \left[k \frac{g}{q_0} \overline{(w'q')}_0 z\right]^{1/3}$
Temperature	$q_* = -\overline{(q'w')}_0 / u_*$	$q_F = \overline{(q'w')}_0 / u_F$
Length	$L = -u_*^3 \Big/ \left(k \frac{g}{q_0} \overline{(w'q')}_0\right)$	z

Where k is the von Karman constant. The Monin-Obukhov similarity should be used when the SL turbulence structure is predominantly sustained by mechanical production and thermal production (or destruction) can have an important role. When the mechanical production is no important and the SL turbulence structure is sustained basically by the thermal production, the Free Convection similarity should by used in the SL.
The Mixed Layer and Local similarities are valid for regions of the PBL well above the SL. The Mixed Layer Similarity has successfully been applied to diagnose the vertical variance of wind velocity components and potential temperature in the convective PBL (Hojstrop, 1982). It is a generalization of the Free Convection similarity to regions above of the

SL where the characteristic length scale z_i is given by the height of the convective PBL (Sorbjan, 1989). In the Mixed Layer, the characteristic scales of wind and temperature and length are, respectively, w_*, Θ_* and z_i (Table 3).

Table 3: Characteristic scales used in the Mixed Layer and Local Similarity valid for the Convective and Stable Planetary Boundary layer.

Characteristic Scale	Mixed Layer	Local
Wind Velocity	$w_* = \left[\frac{g}{q_0}(\overline{w'q'})_0 z_i\right]^{1/3}$	$u_E = \sqrt[4]{(\overline{u'w'})^2 + (\overline{u'w'})^2}$
Temperature	$Q_* = (\overline{q'w'})_0 / w_*$	$q_E = -(\overline{q'w'})/u_E$
Length	z_i	$L = -u_E^{\,3} \Big/ \left[k\frac{g}{q_0}(\overline{q'w'})\right]$

The Local Similarity was developed by Nieuwstadt (1984) and used to PBL under stable conditions (occurring during nighttime over continental areas) when the turbulence is continuous. It can be understood as a generalization of the Monin-Obukhov Similarity to regions above the SL where the characteristic scales of wind, temperature and length – respectively, u_E, q_E, and L - are estimated in terms of the local values of vertical turbulent fluxes of sensible heat and horizontal wind (Table 3). This particularity confers to the Local Similarity the Z-Less characters (Wyngaard, 1985).

2.2 Bulk Models

The bulk models are based on the integrated version of the motion equations (Table 4) assuming that when the intensity of the vertical turbulent mixing is large the mean properties of the flow are vertically homogeneous in large portion of the PBL. This is typically found over the continental areas and during daytime period. However, intense vertical turbulent mixing can be found during nighttime over continental areas due to large horizontal wind but it is a much less frequent situation.

Table 4: Equations used in the bulk models.

	Bulk Equation	Unknowns
1	$\frac{\partial \overline{u}_M}{\partial t} = -\frac{\left[(\overline{u'w'})_i - (\overline{u'w'})_0\right]}{h} + f\left(\overline{v}_M - \overline{v}_g\right)$	$\overline{u}_M$
2	$\frac{\partial \overline{v}_M}{\partial t} = -\frac{\left[(\overline{v'w'})_i - (\overline{v'w'})_0\right]}{h} - f\left(\overline{u}_M - u_g\right)$	$\overline{v}_M$
3	$\frac{\partial \overline{q}_M}{\partial t} = -\frac{\left[(\overline{q'w'})_i - (\overline{q'w'})_0\right]}{h}$	$\overline{q}_M$
	Entrainment Layer Equation	
4	$\frac{\partial D\overline{u}}{\partial t} = \frac{\left[(\overline{u'w'})_i - (\overline{u'w'})_0\right]}{h} + fD\overline{v}$	$D\overline{u}$
5	$\frac{\partial D\overline{v}}{\partial t} = \frac{\left[(\overline{v'w'})_i - (\overline{v'w'})_0\right]}{h} - fD\overline{u}$	$D\overline{v}$
6	$\frac{\partial D\overline{q}}{\partial t} = \frac{\partial h}{\partial t}g_q + \frac{\left[(\overline{q'w'})_i - (\overline{q'w'})_0\right]}{h}$	$D\overline{q}$
	PBL height Equation	
7	$\frac{\partial h}{\partial t} = -\frac{(\overline{q'w'})_i}{D\overline{q}} = -\frac{(\overline{u'w'})_i}{D\overline{u}} = -\frac{(\overline{u'w'})_i}{D\overline{v}}$	h
	Closure	
8	$-\frac{(\overline{q'w'})_i}{(\overline{q'w'})_0} = -\frac{(\overline{u'w'})_i}{(\overline{u'w'})_0} = -\frac{(\overline{u'w'})_i}{(\overline{u'w'})_0} = b$	$(\overline{q'w'})_0$, $(\overline{u'w'})_0$, $(\overline{v'w'})_0$

The closure problem is overcome, in the case of the bulk models, by using the turbulent kinetic energy equation and considering similarity laws for convective case (Deardorff, 1980, Wyngaard, 1989). The bulk model is very easy to implement numerically and admits analytical solution to estimate the height of the convective PBL (Oliveira et al,

1998): $h(t)=\sqrt{\left(14\int_{t_0}^{t}(\overline{q'w'})_0\,dt\right)\Big/(5g_q)}$, where the symbols used here are described in Figs 1 and 2. Besides it can be used as tool to understand the behavior of the well mixed PBL.

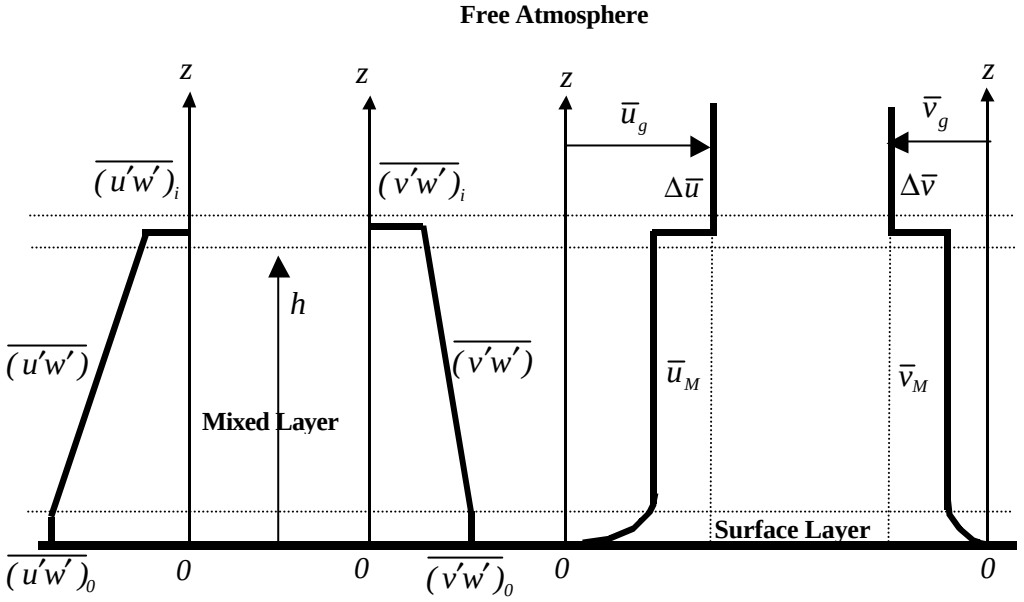

Figure 2: Schematic description the bulk model dynamic structure for convective PBL. The vertical extent of the PBL is indicated by h. The mixed layer horizontal wind components are indicated by $\overline{u}_M$ and $\overline{v}_M$. The vertical turbulent fluxes of the components of horizontal wind at the top of the mixed layer are indicated by $\overline{(u'w')}_i$ and $\overline{(v'w')}_i$. The respective wind shear across the entrainment layer are indicated by $\Delta\overline{u}=\overline{u}_g(h+\varepsilon/2)-\overline{u}_M$ and $\Delta\overline{v}=\overline{v}_g(h+\varepsilon/2)-\overline{v}_M$.

2.3 First Order Closure

The first order closure model of the PBL is based on the analogy between turbulent and molecular transports of the property. Therefore, the PBL turbulent fluxes can be written as given in Table 5, where K_M and K_H are, respectively, the momentum and heat coefficients of turbulent diffusivity in the vertical direction.

Table 5: Equations used in the first order closure models.

	Equation	Unknown
1	$\frac{\partial\overline{u}}{\partial t}=\frac{\partial}{\partial z}\left(K_M\frac{\partial\overline{u}}{\partial z}\right)+\left(-\frac{1}{\rho_o}\frac{\partial\overline{p}}{\partial x}+f\overline{v}\right)$	$\overline{u}$, K_M
2	$\frac{\partial\overline{v}}{\partial t}=\frac{\partial}{\partial z}\left(K_M\frac{\partial\overline{v}}{\partial z}\right)+\left(-\frac{1}{\rho_o}\frac{\partial\overline{p}}{\partial y}-f\overline{u}\right)$	v, K_M
3	$\frac{\partial\overline{q}}{\partial t}=\frac{\partial}{\partial z}\left(K_H\frac{\partial\overline{q}}{\partial z}\right)$	$\overline{q}$, K_H

The number of expressions used to estimate K_M and K_H in the atmospheric applications is very large (Holt and Raman, 1988) and most of them are based on the mixing length approach (Table 6). While they have gained a great popularity among the modeling community in the 60's and yearly 70's, the first order closure model based on parameterizations of K_M and K_H in terms of mixing length and mean properties has been progressively substituted by parameterizations taking into consideration the turbulent kinetic energy equation (Table 7).

Table 6: First order closure model based on mixing length (l) approach.

Closure	
$K_M=l^2\left[\left(\frac{\partial\overline{u}}{\partial z}\right)^2+\left(\frac{\partial\overline{v}}{\partial z}\right)^2\right]^{1/2}$	l

$K_H = K_M / Pr$	Pr Turbulent Prandtl number
$\frac{1}{l} = \frac{1}{\kappa z} + \frac{1}{l_o}$	l_0
$l_0 = c_0 \frac{\left(\bar{u}_g^{\,2} + \bar{v}_g^{\,2}\right)^{1/2}}{\lvert f \rvert}$ $c_0 = 2.7\ 10^{-4}$	

Table 7: First order closure model based on turbulent kinetic energy equation (1 1/2 order closure).

Closure	
$\frac{\partial \bar{e}}{\partial t} = K_M \left[\left(\frac{\partial \bar{u}}{\partial z} \right)^2 + \left(\frac{\partial \bar{v}}{\partial z} \right)^2 \right] - \frac{g}{\theta_0} K_H \frac{\partial \bar{\theta}}{\partial z} - e_2 \frac{\bar{e}^{3/2}}{l_e} + e_1 \frac{\partial}{\partial z} \left(K_M \frac{\partial \bar{e}}{\partial z} \right)$ where $e_1 = 1.2$, $e_2 = 0.125$ and l_e is the dissipation length scale given by Therry and Lacarrère (1983)	e, $\bar{u}$, K_M, K_H
$K_M = Pr\ K_H = c_k l \sqrt{e}$ $\quad Pr$ is the turbulent number of Prandtl and $c_K = 0.4$.	l_K
$\frac{1}{l} = \frac{1}{\kappa (z + z_0)} + \frac{C_{e1}}{h_i} - \left(\frac{1}{\kappa z} + \frac{C_{e2}}{z_i} \right) m_1 m_2 + \frac{C_{e5}}{l_s}$, where $m_1 = \left(1 + C_{e3}\, z_i / \kappa z\right)^{-1}$ $m_2 = \begin{cases} 0 & L \geq 0 \\ \left(1 + C_{e4}\, L / \kappa z\right)^{-1} & L < 0 \end{cases}$ $\frac{1}{l_s} = \begin{cases} 0 & \partial \bar{\theta} / \partial z \leq 0 \\ \left(\frac{g}{\theta_0} \frac{\partial \bar{\theta}}{\partial z} \Big/ \hat{e} \right)^2 & \partial \bar{\theta} / \partial z > 0 \end{cases}$ The constants C_{ei} are determined experimentally, and the boundary layer height z_i is defined as the height at which the profile of turbulent energy e first falls to 5 % of its surface value.	

An example of numerical simulation of PBL vertical structure is given in the Fig. 3. The vertical profile of potential temperature indicates a mixed layer about 750 m deep and the vertical extent of the PBL can be identified in the vertical profile of turbulent kinetic energy. These results are obtained using the mesoscale model TVM (Martin *et al.*, 2001). The TVM is a three-dimension model which takes into consideration topography and land use of the surface.

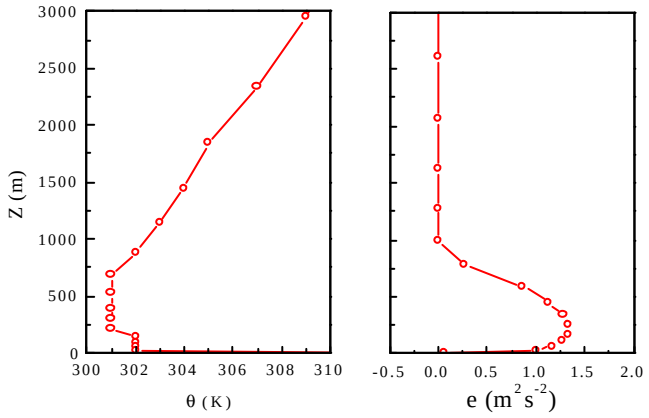

Figure 3: Vertical profile of temperature and turbulent kinetic energy simulated numerically using first order closure coupled to turbulent kinetic energy equation (TVM model). The profile corresponds the 12:00 LT in Iperó, São Paulo, during winter (Karam, *et al.*, 2001).

2.4 Second Order Closure Model (SOCM)

The second order closure models are based on the set of equations that describe the second order statistical moments for momentum and temperature. The second order closure is carried for four terms: third order statistical momentum (or

turbulent fluxes of second order statistical moments); pressure-velocity fluctuations correlation; tendency toward isotropy and molecular dissipation. In general, the parameterization of all these terms requires a particular mixing length. To overcome this problem, Mellor and Yamada (1982) assumed all mixing lengths proportional to the master length scale, where the constants of proportionality are empirically determined from turbulent flows in laboratory. In Table 8 it is described the set of 12 equations and unknowns. In the parameterization used in SOCM, "e" is twice the turbulent kinetic energy; τ_{IM} and τ_{IT} are, respectively, the characteristic time scales for tendency toward isotropy of variance and covariance of momentum and temperature; τ_{DM} and τ_{DT} are, respectively, the characteristic time scales for molecular dissipation of variance of momentum and temperature; K_M and K_H are the coefficients of turbulent diffusion of variance and covariance of momentum and temperature. These scales and coefficients are evaluated in terms of a master length scale. In SOCM the master length, l, is derived from Blackadar mixing-length expression for neutral conditions where the stability effect is introduced *ad hoc* by assumptions on the Blackadar expression (Holt and Raman 1988). According to Mellor and Yamada (1982), the determination of master length scale is the major weakness, precluding a more generic application of SOCM. The most relevant parameters and expressions used in the second order closure model is given in Table 9.

Table 8: Set of equations used in the SOCM developed by Mellor and Yamada (1982).

	Equation	Unknown
1	$\frac{\partial \bar{u}}{\partial t} = -\frac{\partial \overline{(u'w')}}{\partial z} + \left(-\frac{1}{\rho_o}\frac{\partial \bar{p}}{\partial x} + f\bar{v} \right)$	$\bar{u}$ and $\overline{(u'w')}$
2	$\frac{\partial \bar{v}}{\partial t} = -\frac{\partial \overline{(v'w')}}{\partial z} + \left(-\frac{1}{\rho_o}\frac{\partial \bar{p}}{\partial y} - f\bar{u} \right)$	$\bar{v}$ and $\overline{(v'w')}$
3	$\frac{\partial \bar{q}}{\partial t} = -\frac{\partial \overline{(q'w')}}{\partial z} - \left(\frac{1}{\rho_0 c_P}\frac{\partial R_N}{\partial z} \right)$	$\bar{q}$ and $\overline{(q'w')}$
4	$\frac{\partial \overline{(u'u')}}{\partial t} = \frac{\partial}{\partial z}\left(K_M \frac{\partial \overline{(u'u')}}{\partial z} \right) + \left(-\frac{3\overline{(u'u')} - e}{3\tau_{IM}} \right) + \left(-\frac{2}{3}\frac{e}{\tau_{DM}} \right) + \left(-2\overline{(u'w')}\frac{\partial \bar{u}}{\partial z} \right)$	$\overline{(u'u')}$, $\overline{(u'w')}$, $\bar{u}$, e, K_M, τ_{DM}
5	$\frac{\partial \overline{(v'v')}}{\partial t} = \frac{\partial}{\partial z}\left(K_M \frac{\partial \overline{(v'v')}}{\partial z} \right) + \left(-\frac{3\overline{(v'v')} - e}{3\tau_{IM}} \right) + \left(-\frac{2}{3}\frac{e}{\tau_{DM}} \right) + \left(-2\overline{(v'w')}\frac{\partial \bar{v}}{\partial z} \right)$	$\overline{(v'v')}$, $\overline{(v'w')}$, $\bar{v}$, e, K_M, τ_{DM}
6	$\frac{\partial \overline{(w'w')}}{\partial t} = \frac{\partial}{\partial z}\left(K_M \frac{\partial \overline{(w'w')}}{\partial z} \right) + \left(-\frac{3\overline{(w'w')} - e}{3\tau_{IM}} \right) + \left(-\frac{2}{3}\frac{e}{\tau_{DM}} \right) + \left(-2\overline{(q'w')}\frac{g}{\rho_o} \right)$	$\overline{(w'w')}$, $\overline{(q'w')}$, e, K_M, τ_{DM}
7	$\frac{\partial \overline{(u'w')}}{\partial t} = \frac{\partial}{\partial z}\left(K_M \frac{\partial \overline{(u'w')}}{\partial z} \right) + \left(-\frac{\overline{(u'w')}}{\tau_{IM}} + c_1 e\frac{\partial \bar{u}}{\partial z} \right) + \left(-\overline{(w'w')}\frac{\partial \bar{u}}{\partial z} + \overline{(q'u')}\frac{g}{\rho_o} \right)$ $c_1 = 0.08$	$\overline{(u'w')}$, $\bar{u}$, e, $\overline{(w'w')}$ $\overline{(q'u')}$, K_M, τ_{IM}
8	$\frac{\partial \overline{(v'w')}}{\partial t} = \frac{\partial}{\partial z}\left(K_M \frac{\partial \overline{(v'w')}}{\partial z} \right) + \left(-\frac{\overline{(v'w')}}{\tau_{IM}} + c_1 e\frac{\partial \bar{v}}{\partial z} \right) + \left(-\overline{(w'w')}\frac{\partial \bar{v}}{\partial z} + \overline{(q'v')}\frac{g}{\rho_o} \right)$	$\overline{(v'w')}$, $\overline{(w'w')}$, $\bar{v}$, e, $\overline{(q'v')}$, K_M, τ_{IM}
9	$\frac{\partial \overline{(q'u')}}{\partial t} = \frac{\partial}{\partial z}\left(K_H \frac{\partial \overline{(q'u')}}{\partial z} \right) + \left(-\frac{\overline{(q'u')}}{\tau_{IT}} \right) + \left(-\overline{(q'w')}\frac{\partial \bar{u}}{\partial z} - \overline{(u'w')}\frac{\partial \bar{q}}{\partial z} \right)$	$\overline{(q'u')}$, $\overline{(q'w')}$, $\bar{u}$, $\overline{(u'w')}$, $\bar{q}$, K_H, τ_{IT}
10	$\frac{\partial \overline{(q'v')}}{\partial t} = \frac{\partial}{\partial z}\left(K_H \frac{\partial \overline{(q'v')}}{\partial z} \right) + \left(-\frac{\overline{(q'v')}}{\tau_{IT}} \right) + \left(-\overline{(q'w')}\frac{\partial \bar{v}}{\partial z} - \overline{(v'w')}\frac{\partial \bar{q}}{\partial z} \right)$	$\overline{(q'v')}$, $\overline{(q'w')}$, $\bar{v}$, $\overline{(v'w')}$, $\bar{q}$, K_H, τ_{IT}
11	$\frac{\partial \overline{(q'w')}}{\partial t} = \frac{\partial}{\partial z}\left(K_H \frac{\partial \overline{(q'w')}}{\partial z} \right) + \left(-\frac{\overline{(q'w')}}{\tau_{IT}} \right) + \left(-\overline{(w'w')}\frac{\partial \bar{u}}{\partial z} + \overline{(q'q')}\frac{g}{\rho_o} \right)$	$\overline{(q'w')}$, $\overline{(w'w')}$, $\bar{u}$, $\overline{(q'q')}$, K_H, τ_{IT}
12	$\frac{\partial \overline{(q'q')}}{\partial t} = \frac{\partial}{\partial z}\left(K_H \frac{\partial \overline{(q'q')}}{\partial z} \right) + \left(-\frac{\overline{(q'q')}}{\tau_{DT}} \right) + \left(-2\overline{(q'w')}\frac{\partial \bar{q}}{\partial z} \right)$	$\overline{(q'q')}$, $\overline{(q'w')}$, $\bar{q}$, K_H, τ_{IT}

Table 9: Second order closure proposed by Mellor and Yamada (1982).

Variable	Expression	Description
K_H/K	0.20	
K_M/K	0.12	
K	$\lambda\sqrt{e}$	Turbulent diffusion coefficient
t_{IT}/t	0.74	
t_{IM}/t	0.92	
t_{DT}/t	10.1	
τ_{DM}/τ	16.6	
t	$\lambda/\sqrt{e}$	PBL characteristic time scale
l	$\left(1/kz + 1/l_o\right)^{-1}$	Master length scale
l_0	$0.10\left(\int_0^h z\bar{e}dz \Big/ \int_0^h \bar{e}dz\right)$	PBL characteristic length scale
e	$\overline{(u'u')}+\overline{(v'v')}+\overline{(w'w')}$	Twice turbulent kinetic energy

Figures 4 and 5 show, as example, vertical profiles of different meteorological parameters generated by numerical simulation using SOCM. The results correspond to the 12:00 LT, in Ipero (23° 25' S and 47° 35' W), São Paulo, during winter.

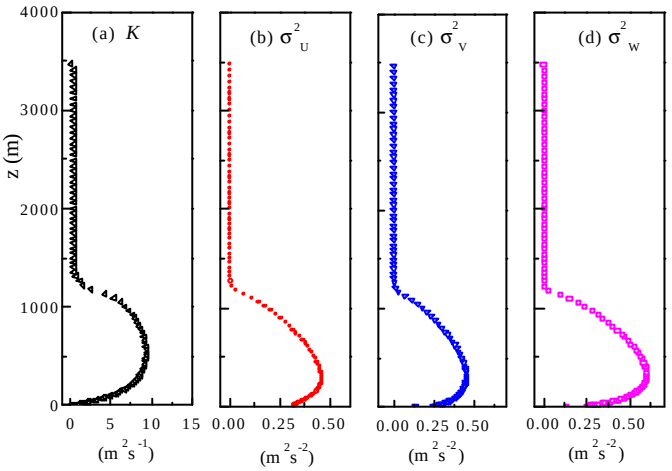

Figure 4: Vertical profiles of (a) diffusion coefficient, (b) variance of zonal, (c) meridional and (d) vertical components of the wind velocity. Numerical simulation using SOCM. The results correspond to the 12:00 LT, in Iperó, São Paulo, during winter:

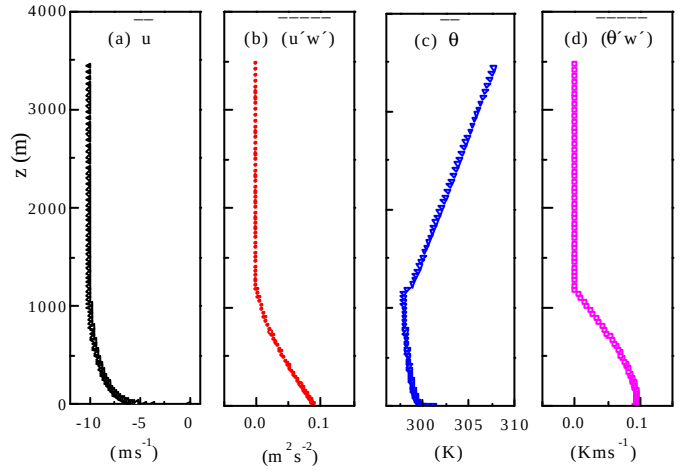

Figure 5: Vertical profiles of (a) zonal component of the wind velocity, (b) vertical turbulent flux of zonal component, (c) potential temperature and (d) vertical turbulent flux of sensible heat flux. Numerical simulation of the PBL by one-dimension SOCM, with 81 grid points in the vertical directions. The results correspond to 12:00LT in Ipero, São Paulo, during winter (Karam, *et al.*, 2001):

2.5 Large Eddy Simulation Model (LES)

In the last 30 years the LES model has been applied to investigate several features of the turbulence in the atmospheric PBL under convective, neutral and stable regimes (Mason, 1994; Lesieur and Métais, 1996). An example of these applications can be seen in Table 10.

Table 10: Characteristics of the LES used to simulate PBL turbulence.

Author	Number of grid points (x, y, z)	Model Domain (x, y, z) (km^3)	Time Step (s)	Total integration time (h)
Deardorff (1972)	40,40,20	4 x 4 x 1	-	-
Deardorff (1974)	40,40,40	5 x 5 x 2	-	8
Moeng (1984)	32,32,40	5 x 5 x 2	3	7
Wyngaard and Brost (1984)	40,40,40	5 x 5 x 2	-	1
Van Haren and Nieuwstadt (1989)	40,40,40	5 x 5 x 2	5	-
Moeng and Wyngaard (1989)	96,96,96	5 x 5 x 2	-	-
Moeng and Sullivan (1994)	96,96,96	5 x 5 x 2	-	3
Andrén (1995)	96,96,96	0.6 x 0.4 x 0.5	-	-
Su *et al.* (1998)	96,96,30	0.192 x 0.192 x 0.6	-	-

In Table 10 one can see that in 90's the LES reached the extraordinary spatial resolution with numerical simulations using grid size of 2 meters and spatial domains with 10^6 grid points (Andrén, 1995; Su *et al.*, 1998). Deardorff (1972) carried out the first simulations of the convective PBL, using LES, and verified that the convective wind velocity (w_*) and the PBL height (z_i) were the characteristic scales that formed the mixed layer similarity (Section 2.1). In these remarkable simulations, Deardorff carried also out estimates of the turbulent diffusion of atmospheric pollutants by following the trajectories of a set of particles released in the PBL. Later on, his results were extensively used to develop a set of atmospheric dispersion parameters intensively applied in Lagrangian Particle Models (Lamb, 1984).

In the LES models, in order to describe the spatial scales of motion larger than a particular cutoff scale it is necessary to apply a low pass filter to the mass, momentum and energy equations. To explicitly describe only motions with length scales larger than a determined valor Δ is convenient to use a low pass filter: $\langle f(x_i,t)\rangle = \int G(x_i - x_i')\, f(x_i',t)\, dx_i'$, where f is any variable and G is a filter function, x_i is the coordinate in the i direction and t is time. The resulting momentum and thermodynamic equations are given in Table 11.

Table 11: Equation of motion used in LES models in tensor notation, where δ_{i3} is de Kronecker delta and ε_{ijk} the Levi-Civita tensor. The vector W_j is the Earth rotation rate and ν_0, and k_0 are, respectively, the kinematics viscosity and thermal diffusivity of the air. The sub-grid turbulence terms are $\tau_{ij} = -(\langle u_i u_j\rangle - \langle u_i\rangle\langle u_j\rangle)$ and $\tau_{qj} = -(\langle q u_j\rangle - \langle q\rangle\langle u_j\rangle)$.

	Equation	Unknown
1	$\frac{\partial\langle u_i\rangle}{\partial t} + \frac{\partial\langle u_j\rangle\langle u_i\rangle}{\partial x_j} = -\frac{1}{\rho_0}\frac{\partial\langle p\rangle}{\partial x_i} - g\delta_{i3} + \frac{\langle\theta\rangle-\theta_0}{\theta_0} g\delta_{i3} - 2\varepsilon_{ijk} W_j \langle u_k\rangle + \frac{\partial}{\partial x_j}\left(\nu_0\frac{\partial\langle u_i\rangle}{\partial x_j} + \tau_{ij}\right)$	$\langle u_i\rangle, \langle p\rangle, \tau_{ij}$
2	$\frac{\partial\langle q\rangle}{\partial t} + \frac{\partial\langle u_j\rangle\langle q\rangle}{\partial x_j} = -\frac{1}{c_P\,\rho_0}\frac{\partial\langle Rn_j\rangle}{\partial x_j} + \frac{\partial}{\partial x_j}\left(k_0\frac{\partial\langle q\rangle}{\partial x_j} + \tau_{qj}\right)$	$\langle q\rangle, \tau_{qj}$
3	$\frac{\partial\langle u_i\rangle}{\partial x_i} = 0$	
4	$-\frac{\langle\rho\rangle-\rho_0}{\rho_0} = \frac{\langle\theta\rangle-\theta_0}{\theta_0}$	$\langle\rho\rangle, \langle\theta\rangle$
5	$\frac{1}{\rho_0}\frac{\partial^2\langle p\rangle}{\partial x_i^2} = -\frac{\partial\langle u_j\rangle}{\partial x_i}\frac{\partial\langle u_i\rangle}{\partial x_j} + \frac{\partial}{\partial x_i}\left(\frac{\partial\tau_{ij}}{\partial x_j}\right) + \frac{g\delta_{i3}}{\theta_0}\frac{\partial(\langle\theta\rangle-\theta_0)}{\partial x_i} - 2\varepsilon_{ijk}W_j\frac{\partial\langle u_k\rangle}{\partial x_i}$	$\langle p\rangle$

To closure the equations (1)-(5) it is used the parameterization proposed by Smagorinsky (1993), where the momentum turbulent diffusivity coefficient, K_M, is assumed to be proportional to the product between the local wind shear and the characteristic length scale, D (Table 12). Similarly, the diffusivity coefficients for sensible heat, K_H, is set equal to the ratio of K_M to the Prandtl number (Table 12).

Table 12: Closure expressions used in the LES model.

	Equation	Unknown
1	$\tau_{ij} = 2K_M \langle S_{ij} \rangle + \frac{1}{3}\tau_{nn}\delta_{ij}$	$\langle S_{ij} \rangle$, τ_{nn}, K_M
2	$\tau_{qj} = K_H \, \partial\langle q \rangle / \partial x_j$	$\langle q \rangle$, K_H
3	$K_M = (cD)^2 S$, c is a constant between 0.0649 and 0.336	S, D
4	$K_H = K_M / Pr$	Pr
5	$\langle S_{ij} \rangle = 1/2\left(\partial\langle u_i \rangle / \partial x_j + \partial\langle u_j \rangle / \partial x_i\right)$	
6	$S^2 = 2\left(\partial\langle u_i \rangle / \partial x_j + \partial\langle u_j \rangle / \partial x_i\right)^2$	
7	$D = \sqrt[3]{(DxDyDz)}$, Dx, Dy and Dz are the grid spacing in the x, y and z direction.	

The results presented hereafter are based on the three-dimensional fields generated after the first 1000 time steps (approximately 0.8 hours), when the CBL has reached an state of equilibrium, using LES model developed by Moeng and Sullivan (1994). It was selected 6 outputs (realizations), separated 200 time steps each, from time step 1000 to 2000.

Figure (6a) shows vertical profiles of horizontal-plane average, for each of the 6 realizations, for the skewness. They also included one vertical profile of an ensemble average of these 6 horizontal-plane averages. The second-order and third-order statistical moments were calculated considering the fluctuations of resolved-scale with respect to the horizontal-plane average.

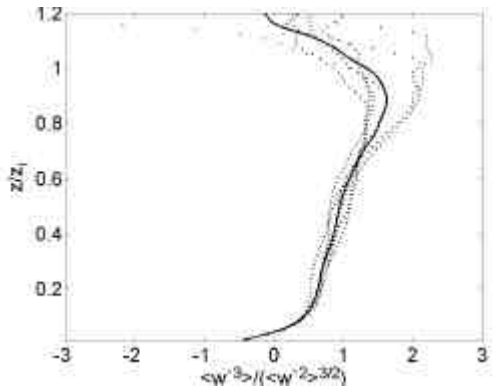

Figure 6a: The vertical profile of the skewness. Numerical simulation using LES with 80^3 grid points in a domain of 5kmx5kmx2km. Forcing and boundary conditions were set to generate highly convective PBL reaching equilibrium for *z/L=-800*.

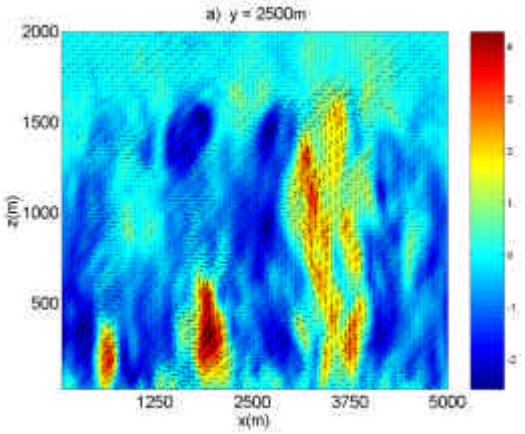

Figure 6b: Contour map of vertical wind velocity in m s^{-1} in a cross section in *y=2500* m. Simulation using LES. For convective conditions. After 1000 time steps.

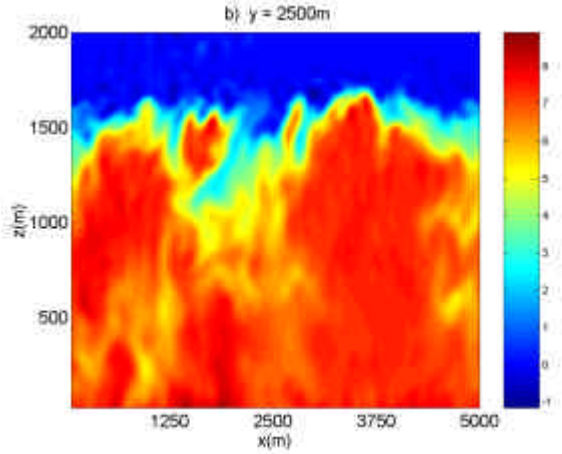

Figure 6c: The contour map of CO concentration (ppm) in a cross section in y=2500 m. Simulation using LES. For convective conditions. After 1000 time steps.

Figures (6b) and (6c) correspond to the instantaneous vertical component velocity and a pollutant concentration fields, simulated after 1000 time steps. In Fig. (6b) it is possible to identify at least one well-defined updraft (region in red and

yellow, between 3000m < x < 3800m. The extensive regions of weak vertical motion are the downdrafts (region in blue). The updraft penetrates the inversion capping inducing descend motion which brings dry and "clean air" of the stable layer above into the CBL. This entrainment of clean air decreases the pollutant concentration near z_i, between 800m < z < 1500 m (Fig. 6c).

3. Conclusion

In this paper the major techniques used to model numerically the PBL are reviewed, and some numerical results are shown. The Monin-Obukhov, Free Convection, Mixed Layer Similarities theories can be applied to diagnose the PBL vertical structure under equilibrium conditions. These four similarities laws can be applied to second order statistic moments and their spectral distribution. Prognostic models are classified in four categories: (a) bulk; (b) first order closure; (c) second order closure and (d) large eddy simulation models. The numerical simulation displayed here indicated that first order closure using turbulent kinetic energy equation is more indicated in most of the meteorological mesoscale models. It combined simplicity and a better physical description of turbulent transport when compared with mixing length approach. The second order closure model is now become a reasonable alternative the first order closure. It required a diagnostic equation for the master length scale on the other hand provides a complete description of the second order moments in the PBL. The large eddy simulation models are considered a research tool available in the investigation of PBL processes, they unravel important features of the PBL structure that are inaccessible to other numerical techniques of modeling. The greatest limitation for LES model application is computational. It requires high performance computers with large I/O capacity. For instance in the simulation displayed here a CRAY J90 took about 4 days of CPU time to simulate 3600 time steps.

4. Acknowledgements

The Authors acknowledge financial support provided by “Conselho Nacional de Desenvolvimento Científico e Tecnológico - CNPq” and by “Fundação de Amparo à Pesquisa do Estado de São Paulo – Fapesp”. The LES model simulations were carried out in the Cray J90 of LCCA/USP.

5. References

Andrén, A., 1995: The Structure of Stably Stratified Atmospheric Boundary Layers: A Large-Eddy Simulation Study. *Quartely Journal Royal Met. Society*, **121(525)**, 961-985.

Avissar, R., Moran, M.D., Wu, G., Meroney, R.N., and Pielke, R. A., 1990: Operating Ranges of Mesoscale Numerical Models and Meteorological Wind Tunnels for the Simulation of Sea and Land Breezes, *Boundary-Layer Meterology*, **50**, 227-275.

Cermak, J. E., 1995: Physical Modeling of Flow and Dispersion over Urban Areas. In: Cermak, J. E.; Davenport, A. G.; Plate, E. J.; Viegas, D. X. Ed. *Wind Climate in Cities*. Kluwer: Dordrecht, Netherlands, 383-403.

Deardorff, J. W., 1972: Numerical Investigation of Neutral and Unstable Planetary Boundary Layers. *Journal of the Atmospheric Sciences*, **29**, 91-115.

Deardorff, J. W. 1974: Three-Dimensional Numerical Study of Turbulence in an Entraining Mixed Layer. *Boundary-Layer Meteorology*, **7**,199-226.

Deardorff, J. W. 1980: Progress in understanding Entrainment at the top of the Mixed Layer, 36-66 *Workshop on Planetary Boundary Layer*, American Meteorological Society, 322 pp.

Dutton, J. A.; Fitchl, G.H., 1969: Approximate Equations of Motion for Gases and Liquids. *Journal of the Atmospheric Sciences*, **26**, 241-254.

Frisch, U., 1995*: Turbulence*, Cambridge, Cambridge Press, 296 pp.

Garratt, J. R.; Hess, G. D.; Physick, W. L.; Bougeault, P., 1996: The Atmospheric Boundary Layer – Advances in Knowledge and Application. *Boundary-Layer Meteorology*, **78**, 9-37.

Hojstup, J, 1982: Velocity Spectra in the Unstable Planetary Boundary Layer. *Journal of Atmospheric Sciences*, **39,** Kaimal, J.C. and J.J. Finnigan, 1994: Atmospheric Boundary Layer Flows, Oxford University Press.

Holt, T. and Raman, S., 1988: A Review and Comparative Evaluation of Multilevel Boundary Layer Parameterizations for First-Order and Turbulent Kinetic Energy Closure Schemes, *Review of Geophysics.*, **26,** 761-780.

Hojstup, J, 1982: Velocity Spectra in the Unstable Planetary Boundary Layer. *Journal of Atmospheric Sciences*, **39,** 2239-48.

Karam, H. A.; Oliveira, A. P.; Pereira, M. M., 2001: R. Application of a Lagrangian Model to Investigate Patterns of Radionuclides Dispersion Over Complex Terrain - Part 1: Local Circulation and Low-Level Jet. *Proceedings of the Seventh International Conference on Harmonization within Atmospheric Dispersion Modeling for Regulatory Purposes*, May 28-31, Belgirate, Italy, 395-399.

Lamb, R. G., 1984: Diffusion in the Convective Boundary Layer In: Nieuwstadt, F. T. M.; van Dop, H. Ed. *Atmospheric Turbulence and Air Pollution Modeling. 1.*ed. Reidel:Dordrecht, 159-229.

Lesieur, M.; Métais, O, 1996: New Trends in Large-Eddy Simulation of Turbulence. *Annual Rev. Fluids Mech.*, **28**, 45-82.

Lu, J.; Arya, S. P., 1995: A Laboratory Simulation of Urban Heat-Island-Induced Circulation in a Stratified Environment. In: Cermak, J. E.; Davenport, A. G.; Plate, E. J.; Viegas, D. X. Ed. *Wind Climate in Cities*. Kluwer: Dordrecht, Netherlands, 405-429.

Mahrt, L., 1986: On the Shallow Motion Approximations. *Journal of the Atmospheric Sciences,* **43(10),** 1036-1044.

Martin, F., S. N. Crespí and M. Palacios, 2001a: Simulation of Mesoscale Circulation in the Center of the Iberian Peninsula for Thermal Low Conditions. Part I: Evaluation of the Topography Vorticity-Mode Mesoscale Model. *Journal of Applied Meteorology*, **40**, 880-904.

Mason, P. J., 1994: Large-Eddy Simulation: A Critical Review of the Technique. *Quarterly Journal Royal Met. Society*, **120**, 1-26.

Mellor, G.L. and Yamada,T., 1982: Development of a Turbulence Closure Model for Geophysical Fluid Problems, *Rev. of Geophys. and Space Phys*., **20**, 851-875.

Moeng, C., 1984: A Large-Eddy-Simulation Model for the Study of Planetary Boundary-Layer Turbulence. *Journal of the Atmospheric Sciences*, **41(13),** 2052-2062.

Moeng, C.; Wyngaard, J. C., 1986: An Analysis of Closures for Pressure-Scalar Covariances in the Convective Boundary Layer. *Journal of the Atmospheric Sciences*, **43(21**), 2499-2513.

Moeng, C.; Wyngaard, J. C., 1989: Evaluation of Turbulent Transport and Dissipation Closures in Second-Order Modeling. *Journal of the Atmospheric Sciences*, .**46(14)**. 2311-2330.

Moeng, C.; Sullivan, P. P., 1994: A Comparison of Shear- and Buoyancy-Driven Planetary Boundary Layer Flows. *Journal of the Atmospheric Sciences*, **51(7),** 999-1022.

Monin. A. S.; Yaglom, A. M., 1971: *Statistical Fluid Mechanics*, Vol. 1, Massachusetts : MIT Press, 769 pp.

Nieuwstadt, F. T. M., 1984a: The Turbulent Structure of the Stable, Nocturnal Boundary Layer. *Journal of the Atmospheric Sciences*, **41(14),** 2202 – 2216.

Oliveira, A.P., Soares, J., Tirabassi, T. and Rizza, U., 1998: A surface energy budget model coupled with a skewed puff model for investigation the dispersion of radionuclides in a Subtropical area of Brazil, *Il Nuovo Cimento*, **21C(6)**, 631-646.

Panofsky, H.A. and J. A. Dutton, 1984: *Atmospheric Turbulence - Models and Methods for Engineering Applications*, John Wiley, New York, 397 pp.

She, Z.; Jackson, E.; Orszag,m 1991: A. Structure and Dynamics of Homogeneous Turbulence: Models and Simulations. *Proc. R. Soc. London*, **434**, 101-124.

Smagorinsky, J., 1993: Some Historical Remarks on the Use of Nonlinear Viscosities. In: Galperin, B.; Orszag, S. A. Ed. *Large Eddy Simulation of Complex Engineering and Geophysical Flows*. 1.ed. Cambridge, 69-106.

Sorbjan, Z, 1989: *Structure of the Atmospheric Boundary Layer*, Prentice, New Jersey, 317 pp.

Stull, R. B., 1988*: An Introduction to Boundary Layer Meteorology*. Dordrecht: Kluwer, 666 pp.

Su, H.; Shaw, R. H.; Paw U, K. T.; Moeng, C.; Sullivan, P. P., 1998: Turbulent Statistics of Neutrally Stratified Flow within and above a Sparse Forest from Large-Eddy Simulation and Field Observations. *Boundary-Layer Meteorology*, **88**, 363-397.

van Haren, L.; Nieuwstadt, F. T. M., 1989: The Behavior of Passive and Buoyant Plumes in a Convective Boundary Layer, as Simulated with a Large-Eddy Model. *Journal Applied Meteorology*, **28**, 818-832.

Wyngaard, J. C., 1984:Boundary Layer Modeling In: Nieuwstadt, F. T. M.; van Dop, H. Ed. *Atmospheric Turbulence and Air Pollution Modeling*. 1.ed. Reidel:Dordrecht, 69-106.

Wyngaard, J. C.; Brost, R. A., 1984:Top-Down and Bottom-Up Diffusion of a Scalar in the Convective Boundary Layer. *Journal of the Atmospheric Sciences*, **41(1**), 102-112.

Wyngaard, J.C., 1985: Structure of the Planetary Boundary Layer and Implications for its modeling, *Journal of Atmospheric Science*, **24**, 1131-1142.